

# Point dynamics model for PWR type reactors

Alan Arsen, Can Ayberk Tekin

*Kungliga Tekniska Högskolan, Department of Nuclear Physics, Stockholm, Sweden*

(Dated: June 4, 2020)

A model for the reactor dynamics of PWR type reactors was implemented using the point kinetic formulation and including the fuel and coolant temperature feedback. A lumped parameters model was used for the fuel and coolant and Newton's law of cooling to account for the heat transfer between them. The parameters used in the model correspond to a TMI-Type PWR. It was evaluated the performance of the model to different transients such as several types of reactivity insertion and external source insertion with and without activating the feedback mechanisms implemented in the model.

Keywords: PWR, Reactor dynamics, temperature feedback, transient

## I. INTRODUCTION

Engineering such a discipline that requires to understand the behaviours of nature, and to manipulate them based on what it is learned from nature for human's interest. Control theory is the main approach to grant this situation. Basically, a system is studied, and specific interventions are determined for the desired outcome. When the desired outcome obtained, this outcome can affect its corresponding intervention naturally or artificially. This phenomenon is defined as feedback, and there are two types of feedback. Positive feedback causes an increase of result, continues this effect under the limits of the system. Negative feedback has a diminishing effect on the outcome. To keep the systems at the desired level, negative feedback mechanisms are used.

Nuclear engineering is one of the applications of the control theory. To produce power at the desired level, a reactivity with a specific magnitude is introduced to the system. The reactivity inputs change the power by affecting reactor kinetics. The power output has a thermodynamic effect on the system. In the end, these thermodynamic effects alter the reactivity by temperature coefficients. Fig. 1 represents a general feedback loop of a power plant.

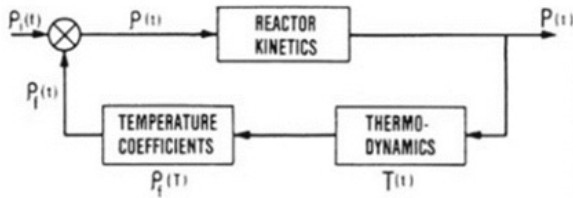


Figure 1. Schematic of the Reactor Dynamics Feedback Loop [1]

In this study, the aim is to investigate feedback behaviour of PWR reactor. In the first part of the study,

point kinetic equations were modelled for a PWR reactor. The required parameters were obtained from a literature survey. The next part focused on specific tasks. The first task was focused on an impulse reactivity input and observed its effects on the system. The next task was implementing an external source to the system and observing the outcomes. After these two tasks, the following group investigated various Doppler feedback coefficients with various step reactivity inputs, and the results were observed. The last group examined various coolant feedback behaviours under negative and positive Doppler feedback coefficients and step inputs. In the end, harmonic reactivity input was introduced to the system, and the stability of the system was analysed. The results were presented in the discussion and conclusions part.

## II. DESCRIPTION OF CALCULATIONS AND NUMERICAL MODELS

In this study, the reactor core dynamics of a PWR type reactor was simulated using the point kinetic model with six groups of precursors and two thermal feedback mechanisms corresponding to fuel and coolant temperature as explained in Sec. II A. The model was implemented in MATLAB and several transients were analysed such as different reactivity insertions with and without the corresponding thermal feedback mechanisms which are presented in Sec. III.

### A. Point Dynamics equations

The general formulation of the point dynamics equations consist of the point kinetics equations and a set of equations describing the non-nuclear phenomena as follows [2]:

$$\frac{dn}{dt} = \left( \frac{\rho - \beta}{\Lambda} \right) n + \sum_i^6 \lambda_i C_i + S, \quad (1)$$

$$\frac{dC_i}{dt} = \frac{\beta_i}{\Lambda} n - \lambda_i C_i, \quad i = 1, \dots, 6, \quad (2)$$

$$\rho = \rho_0 + \rho_C(t) + \sum_{k=1}^K \alpha_k u_k, \quad (3)$$

$$\frac{du_k}{dt} = f_k(n, u_1, u_2, \dots, u_k). \quad (4)$$

Equations 1 and 2 correspond to the point kinetics model where  $n$  is the neutron density,  $\rho$  is the reactivity,  $\beta$  is the effective delayed neutron fraction,  $\Lambda$  is the prompt neutron generation time,  $\lambda_i$ ,  $\beta_i$  and  $C_i$  the decay constant, the effective delayed neutron fraction and the concentration of the precursor  $i$  and  $S$  is the external source. Equation 3 expresses all the different contributions to the reactivity where  $\rho_0$  is the initial reactor reactivity,  $\rho_C(t)$  is the reactivity change due to the control system and the last term corresponds to the changes in reactivity imposed by non-nuclear parameters  $u_k$ , each of them having a reactivity coefficient  $\alpha_k$  associated.

For the present study, only two non-nuclear parameters were considered, namely fuel and coolant temperature. A lumped parameter approach was implemented where the fuel and coolant are represented by a single temperature  $T_F$  and  $T_C$  respectively with their corresponding reactivity coefficients  $\alpha_T^F$  and  $\alpha_T^C$ . A scheme of the modeled system is presented in Fig. 2 where  $W_c(t)$  is the mass flow rate of the coolant and  $T_{Cin}$  and  $T_{Cex}$  are the inlet and exit temperature of the coolant.

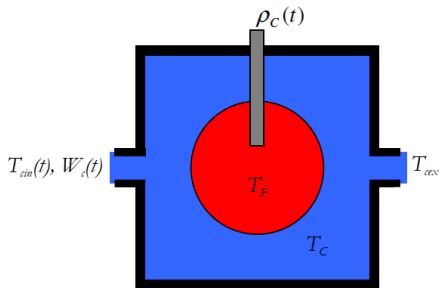


Figure 2. Schematics of the point reactor dynamics model with reactivity, coolant inlet temperature and coolant mass flow rate as external forcing functions [2].

The heat transfer between the fuel and the coolant was implemented using the Newton's equation for cooling with which the heat balance in the fuel and coolant can be expressed as:

$$m_F c_{pF} \frac{dT_F}{dt} = a_F n - h(T_F - T_C), \quad (5)$$

$$m_C c_{pC} \frac{dT_C}{dt} = h(T_F - T_C) - W_c c_{pC} (T_{Cex} - T_{Cin}). \quad (6)$$

Here  $m_F$  and  $m_C$  are the mass of fuel and coolant in the core,  $c_{pF}$  and  $c_{pC}$  are the specific heat of fuel and coolant,  $h$  is the heat transfer coefficient between fuel and coolant,  $a_F$  the power to neutron density ratio and  $T_C$  is obtained as:

$$T_C = \frac{1}{2}(T_{Cex} + T_{Cin}). \quad (7)$$

With these last equations the system of equations is complete and it can be solved if initial conditions are provided. For all the cases analysed in this study, the reactor was considered to be operating in critical condition before the transient started, in other words  $\rho = 0$  and  $n \neq 0$ . Under this conditions, the equilibrium parameters are found to be:

$$n_e = - \frac{\rho_0 + (\alpha_T^C + \alpha_T^F) T_{Cin,e}}{a_F \left[ \frac{1}{2W_{C,e} c_{pC}} (\alpha_T^C + \alpha_T^F) + \frac{\alpha_T^F}{h} \right]}, \quad (8)$$

$$C_{ie} = \frac{\beta_i}{\lambda_i \Lambda} n_e, \quad (9)$$

$$T_{F,e} = T_{Cin,e} + \left( \frac{1}{2W_{C,e} c_{pC}} + \frac{1}{h} \right) a_F n_e, \quad (10)$$

$$T_{C,e} = T_{Cin,e} + \frac{a_F n_e}{2W_{C,e} c_{pC}}. \quad (11)$$

To simplify the numerical implementation, for this study normalised variables were used for the parameters of interested defined as:

$$V_{norm} = \frac{V - V_e}{V_e}, \quad (12)$$

where  $V$  is the original parameter and  $V_e$  the equilibrium value of it. With this normalization, all the initial conditions become zero.

## B. Model parameters

After the PWR point kinetic model was set to use for the project, the next task was to choose the set of parameters for a realistic model. For this situation, a literature survey was performed, and the parameters for a TMI-Type PWR were selected for this project.[3] The parameters are presented in Table I.

Table I. Parameters of a TMI type PWR at the middle of the fuel cycle

|   |  |   |
|---|--|---|
| $a_F = 12.5 \frac{\text{MW}}{\text{m}^3}$ | $T_{C,e} = 302.2^\circ\text{C}$                  | $\beta = 0.006019$                          |
| $c_{pC} = 4200 \frac{\text{W}}{\text{K}}$ | $T_{Cin} = 290^\circ\text{C}$                    | $\Lambda = 0.0002 \text{ s}$                |
| $f = 0.98$                                | $T_{F,e} = 673.8^\circ\text{C}$                  | $\lambda = 0.150 \text{ s}^{-1}$            |
| $h = 6.7 \frac{\text{MW}}{\text{K}}$      | $W_{ce} = 24285 \frac{\text{kg}}{\text{s}}$      | $\mu_C = 71.8 \frac{\text{MW s}}{\text{K}}$ |
| $M = 102 \frac{\text{MW}}{\text{K}}$      | $\alpha_T^C = -21.3 \frac{\text{pcm}}{\text{K}}$ | $\mu_F = 26.3 \frac{\text{MW s}}{\text{K}}$ |
| $P_0 = 2500 \text{ MW}$                   | $\alpha_T^F = -3.24 \frac{\text{pcm}}{\text{K}}$ | $\Omega = 6.6 \frac{\text{MW}}{\text{K}}$   |

Here  $f$  is the fraction of reactor power deposited in the fuel,  $M$  is mass flow rate multiplied by the heat capacity of the coolant,  $P_0$  is initial equilibrium power,  $\mu_C$  is the total heat capacity of the reactor coolant (weight of coolant times its specific heat),  $\mu_F$  is the total heat capacity of the fuel (weight of fuel times its specific heat),  $\Omega$  is heat transfer coefficient between fuel and coolant.

The model which the literature used was slightly different from the model used in this project. Therefore, it was aimed to equalize these two models at the identical operation mode. The chosen reference point was a full-power operation in the middle of the fuel cycle. The lumped parameters of the literature were functions of the neutron density relative to the initial equilibrium density. At full power level, this parameter equals to 1. Thus, the normalized kinetic model was arranged to the full power level and equilibrium neutron density.

To obtain relevant parameters for the normalized point kinetic equation, initial equilibrium fuel temperature and initial average reactor coolant temperature equations were compared for both the literature model eq. (13,14) and the project model eq. (10,11). The equations from the literature were:

$$T_{F,e} = T_{Cin,e} + \left( \frac{1}{2M} + \frac{f}{\Omega} \right) P_0, \quad (13)$$

$$T_{C,e} = T_{Cin,e} + \frac{P_0}{2M}. \quad (14)$$

The equations 13 and 14 were identical equations (10,11) which the study used. Therefore, corresponding

parameters were considered identical and introduced to the system.

The exceptional thing in the parameters, generation time parameter seemed out of the thermal range. Generation time for a thermal zone range was chosen based on the literature [4].

After the parameters were introduced to the code, six groups delayed neutrons and their decay constants were implemented to the system. Parameters were appropriate for the middle of the fuel cycle and they were presented as a table II.

Table II. Six Group Delayed Neutron Group Parameters for Middle of the Fuel Cycle

| $\beta_i$                            | $\lambda_i [\text{s}^{-1}]$ |
|--------------------------------------|-----------------------------|
| 0.0001745                            | 0.01255                     |
| 0.001257                             | 0.0307                      |
| 0.0011405                            | 0.1165                      |
| 0.0023495                            | 0.3125                      |
| 0.000821                             | 1.1900                      |
| 0.0002765                            | 3.15                        |
| $\beta=0.006019 \quad \lambda=0.150$ |                             |

## III. RESULTS

### A. point kinetics simulations

In this section of the study, the behaviour of the point dynamics model at zero power condition was analysed. There were two cases in the study. The first case was an analysis of an impulse reactivity change to the system. The second case was an analysis of a step reactivity change to the system. Thermal feedback mechanisms were not included in this part of the study.

#### 1. Reactivity impulse transient

To introduce an impulse reactivity with magnitude  $\beta$  to the system, a triangular function which has one second residence time was inserted to the system at  $t=0$  while the system was in equilibrium. In the short term, an immediate increase of neutron density, and fuel temperature was observed. After the system reached its equilibrium state, neutron density, precursor densities and temperatures have higher values at their new equilibrium states. Insertion of the reactivity was presented Fig.3

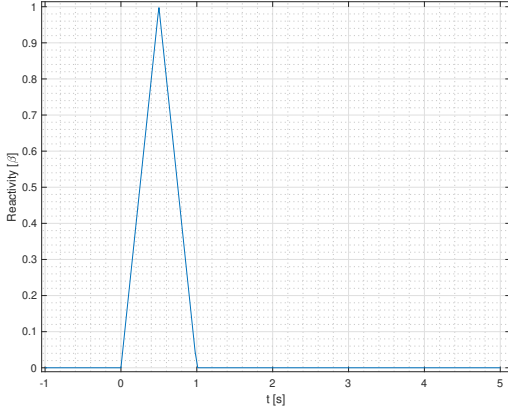


Figure 3. Short term outcome of the reactivity of the system after a positive impulse insertion of external reactivity.

The neutron density was presented in the Fig 4. The increase of the neutron density could be observed in the new equilibrium.

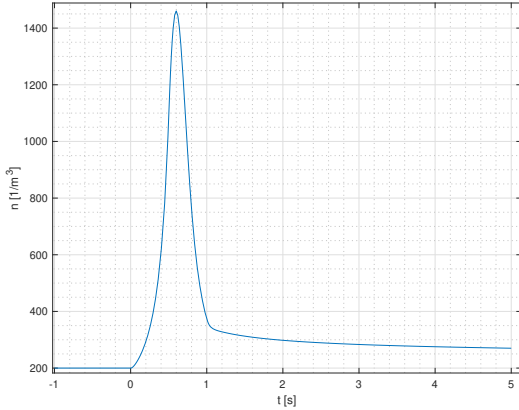


Figure 4. Short term behaviour of the neutron density after a positive impulse insertion of external reactivity.

## 2. External neutron source transient

In this part of the study, an external neutron source was introduced to the system at  $t=0$  while the system was in equilibrium. A continuous linear increase of neutron population and temperature increase was observed till a physically infeasible level. The neutron population of this case was presented Fig 5.

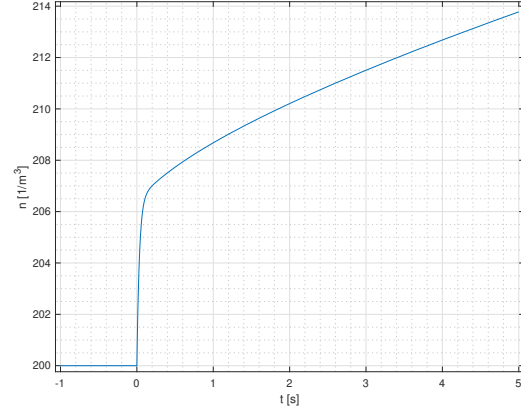


Figure 5. Short term behaviour of the neutron density after an external neutron source was introduced to the system.

## B. Simulations with Doppler feedback

In this section of the study, the behaviour of the point dynamics model with Doppler feedback mechanism was analysed for step reactivity input for various conditions. There were four cases in this section. The first two cases were evaluated respectively negative and positive Doppler feedback coefficients with a beta magnitude step reactivity input while the system in equilibrium.

### 1. Positive reactivity step transient with negative Doppler feedback

In this case, a positive reactivity step magnitude  $\beta$  was introduced to the system had a negative Doppler feedback which means an increase of the fuel temperature led to decreasing reactivity. The reactivity reached its initial equilibrium state after a hundred seconds. The Doppler feedback immediately affected the system. At  $t=3$  s, the reactivity was slightly bigger than the initial equilibrium. This slight reactivity affected precursor concentrations. As a result, a temperature increase was observed between ten and a hundred seconds after the step increase. After a hundred second the reactivity reached its original equilibrium state. Then, the neutron and precursor populations and fuel temperatures became stable. Fig. 6 illustrated the temperature change while the enhanced concentrations of precursors affected the system as presented in Fig. 7

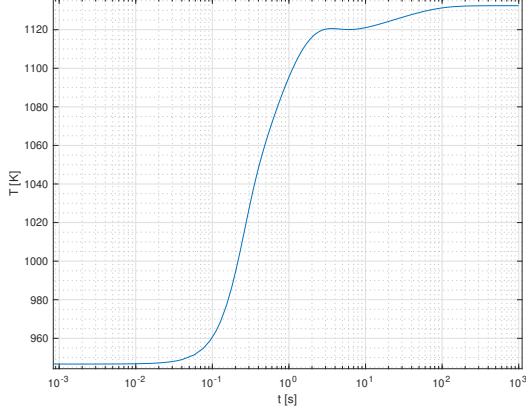


Figure 6. Long term outcome of the fuel temperature after a positive step insertion of external reactivity with negative Doppler feedback.

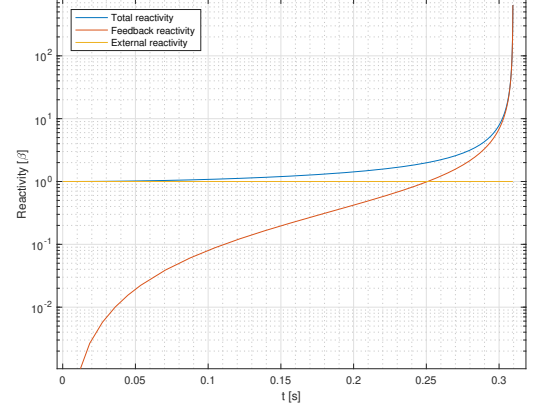


Figure 8. Long term result of the reactivity of the system after a positive step insertion of external reactivity with positive Doppler feedback.

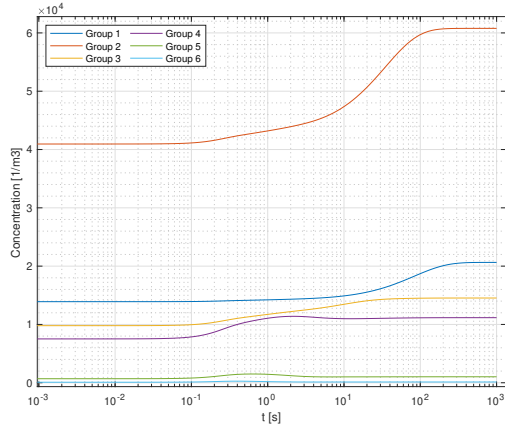


Figure 7. Long term behaviours of the precursor concentrations after a positive step insertion of external reactivity with negative Doppler feedback.

## 2. Positive reactivity step transient with positive Doppler feedback

In this stage, a step reactivity with  $\beta$  magnitude was introduced to the system at  $t=0$  in the equilibrium state. In this case, the Doppler feedback was positive. This situation was similar to Sec. III A 2. However, the response was an exponential increase, and the situation immediately became physically unfeasible. The short term behaviour of the reactivity insertion and the corresponding positive Doppler feedback was illustrated as in the Fig.8.

## 3. Negative reactivity step transient with negative Doppler feedback

In this part, a step reactivity with  $-\beta$  magnitude was introduced to the system at  $t=0$  in the equilibrium state. The negative Doppler feedback has a sufficient magnitude that precursors had an opportunity to slightly increase the neutron population since the precursor concentration started to decrease one second after the neutron population. Thousand seconds later from the initial event, the system reached a new equilibrium with a decreased neutron population. The short term reactivity behaviour after the insertion was expressed in the Fig.9.

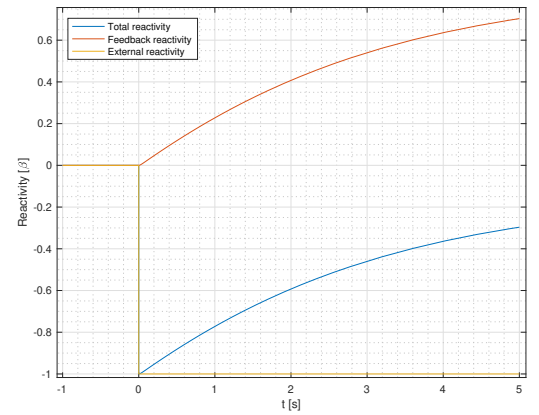


Figure 9. Short term result of the reactivity of the system after a negative step insertion of external reactivity with negative Doppler feedback.

Due to the magnitude of the negative feedback, the system earned a new equilibrium state as in Fig. 10

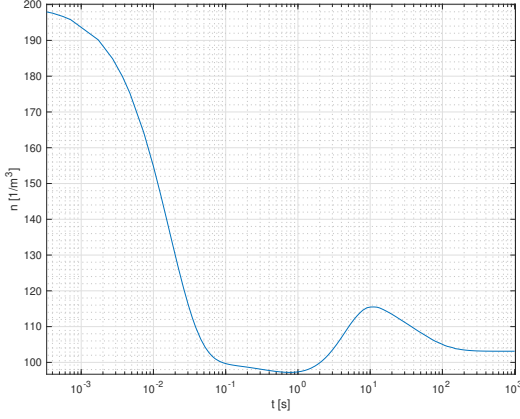


Figure 10. Long term behaviour of the neutron concentration after a negative step insertion of external reactivity with negative Doppler feedback.

This case also had a specific situation. The small magnitude of negative Doppler  $-1.5 \text{ pcm/K}$  coefficient was investigated. In this case, the magnitude of the feedback was not sufficient to operate the reactor. Eventually, the reactor spontaneously shutdown. This phenomenon presented in Fig.11

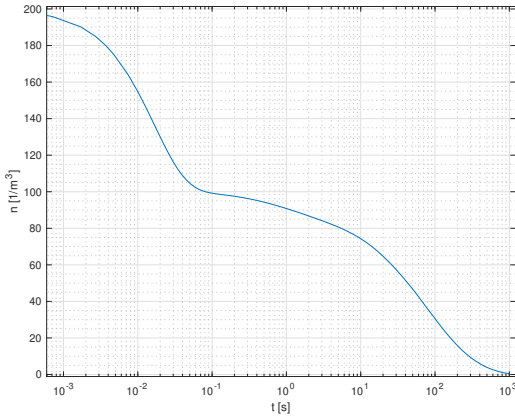


Figure 11. Long term result of the neutron concentration after a negative step insertion of external reactivity with negative Doppler feedback  $-1.5 \text{ pcm/K}$ .

#### 4. Negative reactivity step transient with positive Doppler feedback

In this part, a step reactivity with  $-\beta$  magnitude was introduced to the system at  $t=0$  in the equilibrium

state. The positive Doppler feedback empowered the reactivity change effect so that the neutron population ceased faster than the previously mentioned case. The reactivity behaviour in the short term and the long term effect of the neutron concentration were presented respective Fig.12, Fig.13.

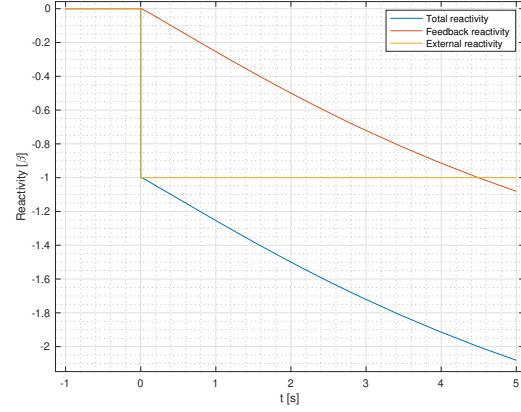


Figure 12. Short term outcome of the reactivity of the system after a negative step insertion of external reactivity with positive Doppler feedback.

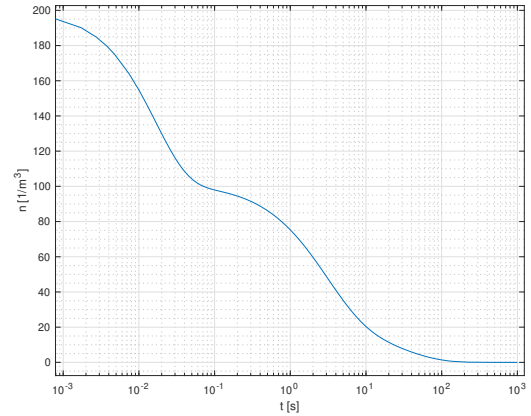


Figure 13. Long term outcome of the neutron concentration after a negative step insertion of external reactivity with positive Doppler feedback.

### C. Complete point dynamics simulations

In this section of the study, the behavior of the complete point dynamics model (including both thermal feedback mechanisms) was analysed for different reactivity insertions, namely step and harmonic oscillations. For both cases, the response of the system was evaluated

with negative Doppler and coolant temperature coefficient. In addition, for the case of the step reactivity insertion, the behavior with positive coolant temperature coefficient was also analysed.

### 1. Reactivity step transient

A positive step of reactivity of magnitude  $\beta$  was introduced at  $t = 0$ , being the system in equilibrium before the transient started. Firstly, the behavior of the reactor with both feedback coefficients negative was analysed. The insertion of the reactivity step as well as the evolution of the total and feedback reactivity of the system is shown in Fig. 14.

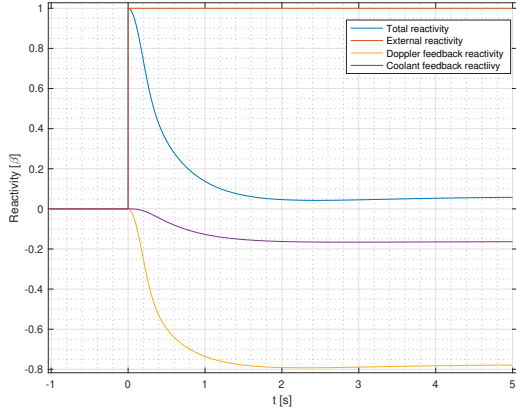


Figure 14. Short term evolution of the reactivity of the system after a positive step insertion of external reactivity.

It can be seen in Fig. 14 the characteristic prompt response of the Doppler feedback that is, with some delay, followed by the coolant temperature feedback. After a few seconds, the thermal transfer from the fuel to the coolant becomes effective, reducing momentarily the fuel temperature and hence leading to a local peak of reactivity at approximately 8 s that can be seen in Fig. 15. After this peak, the systems recovers a steady state condition at about 300 s.

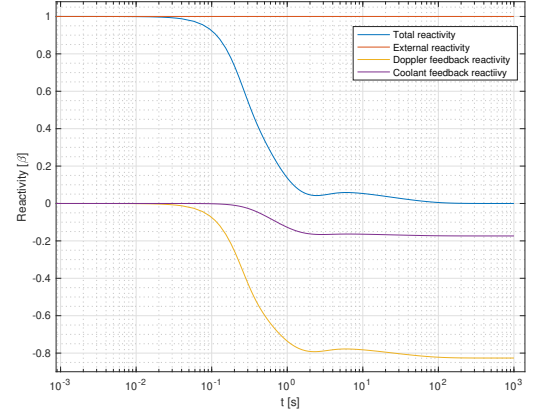


Figure 15. Long term evolution of the reactivity of the system with both feedback coefficients negative after a positive step insertion of external reactivity.

The long term evolution of the reactivity for the case with positive coolant feedback is shown in Fig. 16. For this case, the final outcome is the same, namely the recovery of the critical condition. However, this is achieved at the cost of a considerable higher fuel temperature to obtain a sufficiently large Doppler feedback.

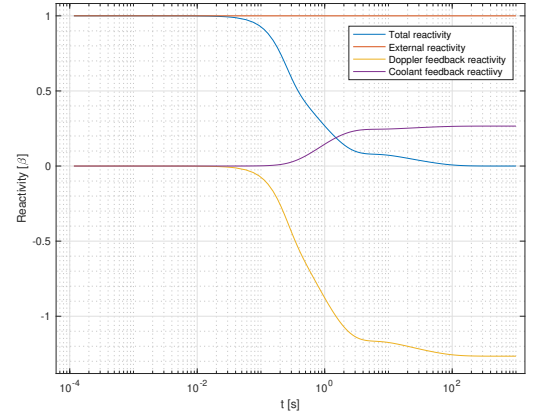


Figure 16. Long term evolution of the reactivity of the system with negative Doppler feedback and positive coolant temperature feedback after a positive step insertion of external reactivity.

This phenomenon can also be seen directly in the evolution of the temperature of the fuel and coolant shown in Fig. 17. Here it can be seen that, as mentioned before, the fuel temperature at the end of the transient is much higher for the case with positive coolant temperature feedback since the Doppler feedback has to compensate both the external reactivity and the coolant feedback. Consequently, the coolant temperature is



slightly higher as well due to the heat transfer between fuel and coolant.

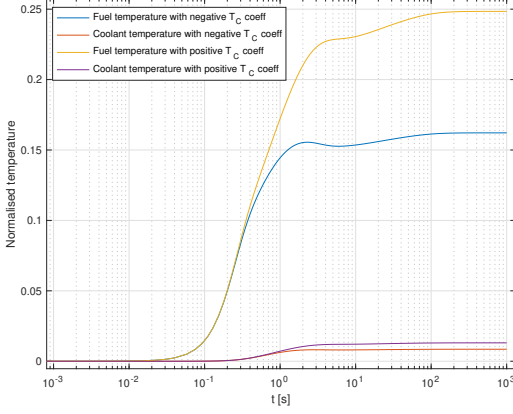


Figure 17. Long term evolution of the of the normalised fuel and coolant temperature after a positive step insertion of external reactivity for the cases with negative and positive  $T_C$  feedback.

The evolution of the neutron population during this transient for both cases is shown in Fig. 18.

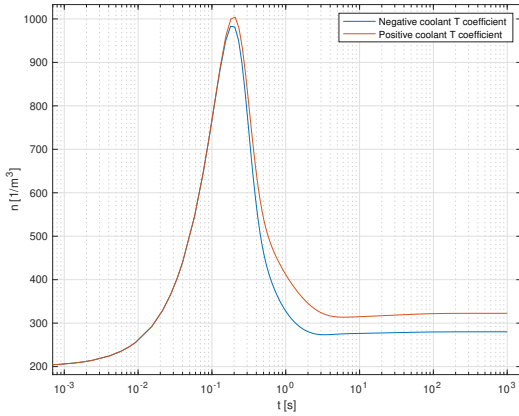


Figure 18. Long term evolution of the neutron population to a positive step insertion of external reactivity for the cases with negative and positive  $T_C$  feedback.

In Fig. 18 it can be seen that for both cases, there is a rapid increase of the neutron population up to about five times its original value in 2 s because of the fast response of the prompt neutrons. Then, it decreases due to the fact that the reactivity of the system is below prompt critical and the precursors are not in equilibrium for that level of neutron population, reaching the new equilibrium level short after the system becomes critical again. It has to be noticed that the new equilib-

rium level is higher for the case of positive  $T_C$  feedback since the rate of decrease of reactivity is slower.

Finally, the evolution of the precursors' concentrations for the case with both negative feedback coefficients are shown in Fig. 19. It is worth mentioning that only one case is presented since the evolution is the same for both cases.

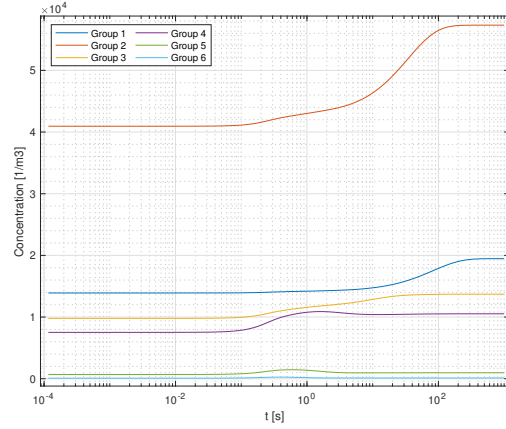


Figure 19. Long term evolution of the of the precursors' concentrations to a positive step insertion of external reactivity.

It can be seen in Fig. 19 that there is a significant delay in the response of the concentrations of precursors to the transient. In particular, it has to be noticed that the change in the aforementioned concentrations during the prompt response is negligible which is compatible with the decrease of the neutron population explained before.

## 2. Harmonic oscillation transient

A symmetric oscillation of reactivity with amplitude  $\beta$  and several frequencies was implemented to the model with both feedback coefficients negative. The evolution of the reactivity of the system to a harmonic oscillation with frequency 0.5 Hz is presented in Fig. 20.



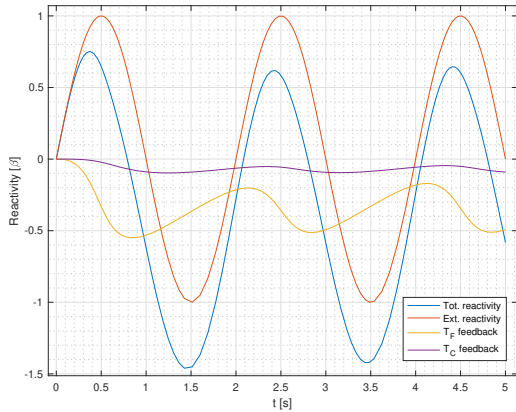


Figure 20. Evolution of the reactivity of the system under a symmetric oscillation of reactivity with frequency 0.5 Hz.

It is worth highlighting that an external symmetric insertion of reactivity converges to a total non-symmetric reactivity oscillation of the system because of the response of the feedback. This is due to the fact that the system responds somehow faster to a positive insertion of reactivity compared to a negative one leading to an average increase in temperature and hence a more negative feedback reactivity. It has to be noticed as well, that in this case the oscillation is slow enough so that the Doppler feedback can, at some extent, impact the overall reactivity from the first period limiting the maximum reactivity of the transient which, in this case, is achieved during the first period.

The evolution of the neutron population to the oscillating reactivity for different frequencies is presented in Fig. 21.

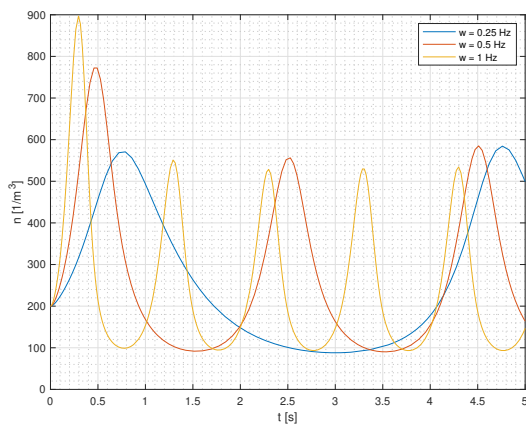


Figure 21. Evolution of the neutron population of the system under a symmetric oscillation of reactivity.

It can be seen in Fig. 21 that the magnitude of the

neutron population during the first period of the transient is highly dependent on the frequency of the oscillation. It was found that, for the set of parameters used, the maximum value of the neutron population is obtained for a frequency around 1 Hz. For lower frequencies, the Doppler feedback is fast enough to compensate more effectively the increase in reactivity. On the other hand, for higher frequencies the system seems to not be capable of following the transient.

Although in Fig. 20 the system seems to be in an equilibrium after a few periods, this is not completely true since it takes considerably longer for the precursors to reach an equilibrium in this condition as shown in Fig. 22, and the fuel and coolant temperature keep increasing slightly to compensate this change.

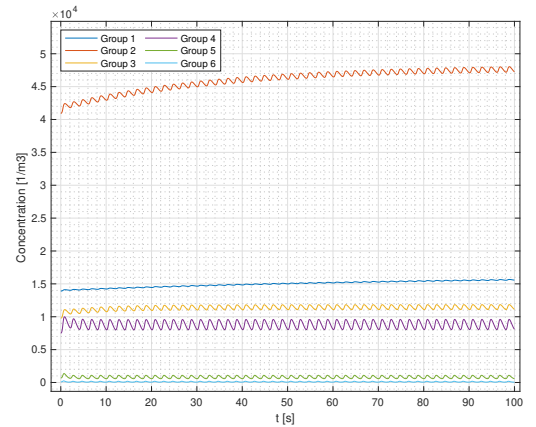


Figure 22. Long term evolution of the precursors' concentration of the system under a symmetric oscillation of reactivity with frequency 0.5 Hz.

#### IV. DISCUSSION AND CONCLUSIONS

In this study, a point dynamics model for PWR types reactor with fuel and coolant feedback mechanisms was successfully implemented. The model was used to investigate the evolution of the relevant parameters to the system under several transient conditions.

The importance of the feedback was revealed by observing multiple transients in various configurations. The feedback behaviors of fuel and coolant temperature have proved to be a crucial aspect for safe operation. Moreover, the precursor effects were observed. They resulted in a slight temperature and neutron population increase in a system.

The effect of the feedback magnitude was noticed in the tasks. A strong response could prevent a spontaneous shut down as in the Sec.III B 3.

In Sec.III C 1, it was observed that the reactor could be operated in principle with a positive coolant temper-

ature feedback coefficient. On the other hand, a positive Doppler feedback has shown to produce severe consequences under transients. In addition, it was observed that a symmetric oscillating reactivity change with feedback lead to a dynamic system equilibrium. It means

the system behaviour was oscillating within expected boundaries as presented Sec.III C 2. It was also found in this part of the study that the final reactivity oscillation is not symmetric showing that the system tends to respond faster to a positive reactivity change compared to a negative one.

- 
- [1] G Kessler. *Sustainable and Safe Nuclear Fission Energy*. Page 49, Springer, 2012.
  - [2] Henryk Anglart. *Nuclear Reactor Dynamics and Stability*. Pages 73-81, 2011.
  - [3] K. Torabi, O. Safarzadeh, and A. Rahimi-Mohaddam. *Robust Control of the PWR Core Power Using Quantitative Feedback Theory*. IEEE Transactions on Nuclear Science, vol. 58, no.1, Pages 260-261, 2011.
  - [4] J.R. Lamarsh, A. J. Baratta. *Introduction to Nuclear Engineering Third Edition* Page 332, 2001.